International Journal of Concrete Structures and Materials
Vol.11, No.4, pp.647–655, December 2017
DOI 10.1007/s40069-017-0214-7
ISSN 1976-0485 / eISSN 2234-1315

Experiments on Tensile and Shear Characteristics of Amorphous Micro Steel (AMS) Fibre-Reinforced Cementitious Composites

Jeong-Su Kim[1)], Chang-Geun Cho[2),*], Hyeong-Joo Moon[2)], Hoyeon Kim[2)], Seung-Jung Lee[2)], and Wha-Jung Kim[3)]

(Received December 19, 2016, Accepted August 21, 2017, Published online December 7, 2017)

Abstract: Amorphous micro-steel (AMS) fibre made by cooling of liquid pig iron is flexible, light and durable to corrosion, then to be compatible with high flowable and disperable states of mixing as well as high ductile post-cracked performances to apply in fibre-reinforced cementitious composites. In the current research, AMS fibre-reinforced cementitious composites based on cement and alkali-activated ground granulated blast furnace slag mortars were newly manufactured and evaluated for the strength and ductile characteristics mainly by direct tensile and shear transfer tests in the variation in the volume of AMS fibres with two different lengths of 15.0 and 30.0 mm. As a result, it was found that 1.0–1.25% fibre volume fractions were recommendable for AMS fibre-reinforced cementitious composites to maximize direct tensile strength, ductile tensile strain, and shear strength of the composites. However, a further fraction of AMS fibre lowered these mechanical characteristics. Simultaneously, it could be said that AMS fibre-reinforced cementitious composites exhibited up to about 3.7 times higher in direct tensile strength and up to 2.3 times higher in shear strength, compared to AMS fibre-free specimens.

Keywords: fibre-reinforced cementitious composites, amorphous micro-steel (AMS) fibre, crack control, tensile strength, shear transfer.

1. Introduction

Attempts to utilize fibre cementitious or concrete composites mixed with metallic or non-metallic fibres had been greatly made in fields of high rise building and infra structures in order to enhance additional requirements of high ductility, performance and durability (Narayanan and Darwish 1987; Ashour et al. 1992; De Hanai and Holanda 2008; Fischer and Li 2003; Kim et al. 2009; Lee et al. 2012; Choi et al. 2014). For fibre-reinforced cementitious composites, non-metallic fibres such as synthetic fibres were used to mainly develop high ductile characteristics after cracking, with no improvement of strength, known as engineered cementitious composites (ECC) or strain-hardening cementitious composites (SHCC) (Fischer and Li 2003; Lee et al. 2012; Choi et al. 2014; Cho et al. 2012; Kim et al. 2014). On the other hand, steel fibres are often used to mix in concrete or cementitious composites to refine their brittle characteristics by enhancing tensile and shear strength (Narayanan and Darwish 1987; Ashour et al. 1992; De Hanai and Holanda 2008; Özgür and Khaled 2009; Özcan et al. 2009; Lim and Hong 2016; Lu et al. 2016).

Most of steel products used in construction fields such as deformed reinforcing bars, steel fibres, and steel plates, etc., in general, are crystalline metals, of which properties are mainly characterized by adjusting the cooling speed after crystalline metals are liquefied under high temperature. A crystal in metal is formed when liquid metal is cooled slowly at thousands of degrees per second (Won et al. 2012; Seo 2006). These crystalline steels are basically an anisotropic material, consisting of regular arrays of atoms, so that their mechanical characteristics are dependent on crystal directions, such as in exhibiting the modulus of elasticity, electrical and heat conductivities, and refractivity.

In the manufacturing process, steel fibres produced from wires are subjected to a repeated heating and cooling process of lengthening and thinning, then to achieve suitable shape, yield and rupture strength as well as elastic modulus. Considering in fibre-reinforced cementitious composites, steel fibre is, however, susceptible to corrosion in a humid atmospheric condition. Moreover, high level of the specific gravity may lower dispersion of steel fibres in fresh binders; a suitable quality of fibre-reinforced cementitious composites may not be achieved (Won et al. 2012; Morga et al. 1999; Yoo et al. 2016).

Amorphous micro-steel is fundamentally different in the manufacturing process that cools liquid pig iron at the bottom of a furnace under fast rotation and do not make

[1)]Hanwha Research Institute of Technology, Hanwha E&C, Daejeon, Republic of Korea.
[2)]School of Architecture, Chosun University, Gwangju, South Korea.
*Corresponding Author; E-mail: chocg@chosun.ac.kr
[3)]School of Architecture, Kyungpook National University, Daegu, South Korea.

crystalline grain boundaries in the metal, when the metal liquid is cooled rapidly above 10^5 K/s (Won et al. 2012; Seo 2006). Therefore, the micro-steel is a pure isotropic as independent to material directions and an amorphous metal as exhibiting liquid characteristics in solid, called as a liquid metal. Amorphous micro-steel has not only a superb strength and toughness with the relatively low specific gravity in mechanical characteristics, but also has distinguished durability to resist corrosion in humidity, acid and exposed atmospheres (Won et al. 2012; Seo 2006). Some researchers attempted to evaluate mechanical properties of mortar or concrete including AMS fibres (Redon and Chermant 1999; Won et al. 2013; Dinh et al. 2016; Yoo et al. 2016).

In this study, the feasibility of a new micro-steel fibre (i.e. amorphous micro-steel fibre made by cooling of liquid pig iron) reinforced cementitious composite based on cement and alkali-activated ground granulated blast furnace slag (GGBS) mortars was experimentally assessed for the strength and ductile characteristics mainly by direct tensile and shear transfer tests in the variation in the volume of AMS fibres with two different lengths of 15.0 and 30.0 mm. In addition to optimize the volume of the steel fibre in the mix, the slump flow, the compressive strength, the direct tensile behavior, and the shear transfer were examined.

2. Amorphous Micro-Steel Fibre-Reinforced Cementitious Composites

2.1 Manufacturing of Fibre-Reinforced Cementitious Composites

Amorphous micro-steel (AMS) fibre can be easily and quickly manufactured by cutting immediately after a rapid cooling process of the amorphous liquid metal, as shown in Fig. 1. Two different AMS fibres (thickness × width × length; 0.028 × 1.0 × 15.0 mm and 0.028 × 1.0 × 30.0 mm) were well dispersed mixed, respectively in mortar of which ratio for ordinary Portland cement (OPC), ground granulated blast furnace slag (GGBS), silica sand, and water was 1.25: 0.31: 1.00: 1.19 by mass. The specific gravity of the steel fibre was equated to 7.0–7.2, and ≥ 1600 MPa in the tensile strength. Simultaneously the oxide composition for OPC and GGBS is given in Table 1. The fraction of AMS fibre was in the range of 0, 0.5, 0.75, 1.00, 1.25 and 1.50% by volume of the mortar. To manifest uniform fibre dispersion, the viscosity modifying admixture (VMA) was added in the mix to achieve adequate rheological property (Cho et al., 2012). Then, slump flow was measured immediately after mixing mortar containing the AMS fibre, and the compressive, tensile and shear strengths were measured after 28 days of curing in water at 23 ± 3 °C.

2.2 Measurement of Slump and Mechanical Tests

The flow and mechanical characteristics of fresh and hardened AMS fibre composite were tested and measured varying with the fibre volume(0, 0.5, 0.75, 1.00, 1.25 and 1.50%) for two different fibre length of L = 15 mm and L = 30 mm. The fluidity of mortar containing AMS fibre was measured immediately after mixing, casting in a cone and removing the cone, of which the taper-shaped margin was Ø100 × Ø200 × 300 mm (KS F 2402 2007). Uniaxial compressive strength was measured by a 50 mm cube specimen for two specimens for each mix, according to ASTM C109-07 (ASTM 2007).

Simultaneously the schematic of specimens for measuring the tensile strength and strain as well as shear strength is given in Fig. 2 (Kim et al. 2007; Mattock and Hawkins 1972). The specimens for the direct tensile test in Fig. 3 were made to have two dog-bone shapes in both ends, as already shown elsewhere (Kim et al. 2007), to avoid fractures outside the gage length. As shown in Fig. 3, the

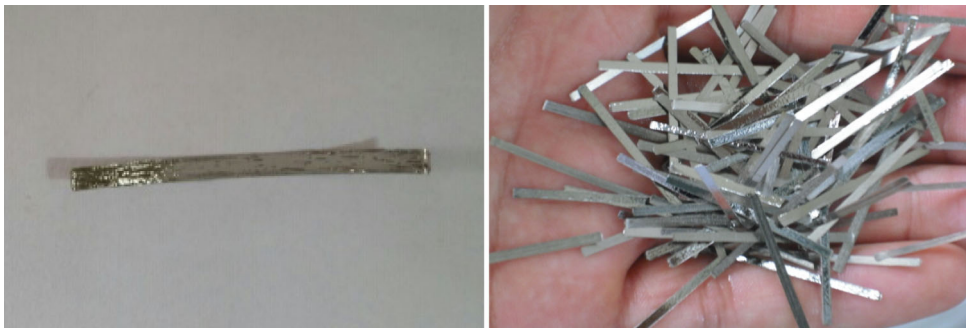

Fig. 1 Photos of amorphous micro steel fibres.

Table 1 Oxide composition of OPC and GGBS.

	SiO_2	Al_2O_3	Fe_2O_3	CaO	MgO	K_2O	TiO_2	SO_3	LOI[a]
OPC	21.2	4.58	2.84	62.3	0.05	0.01	–	2.01	0.58
GGBS	34.7	13.8	0.11	44.6	4.38	0.48	0.74	0.95	0.24

[a] Loss of ignition (%).

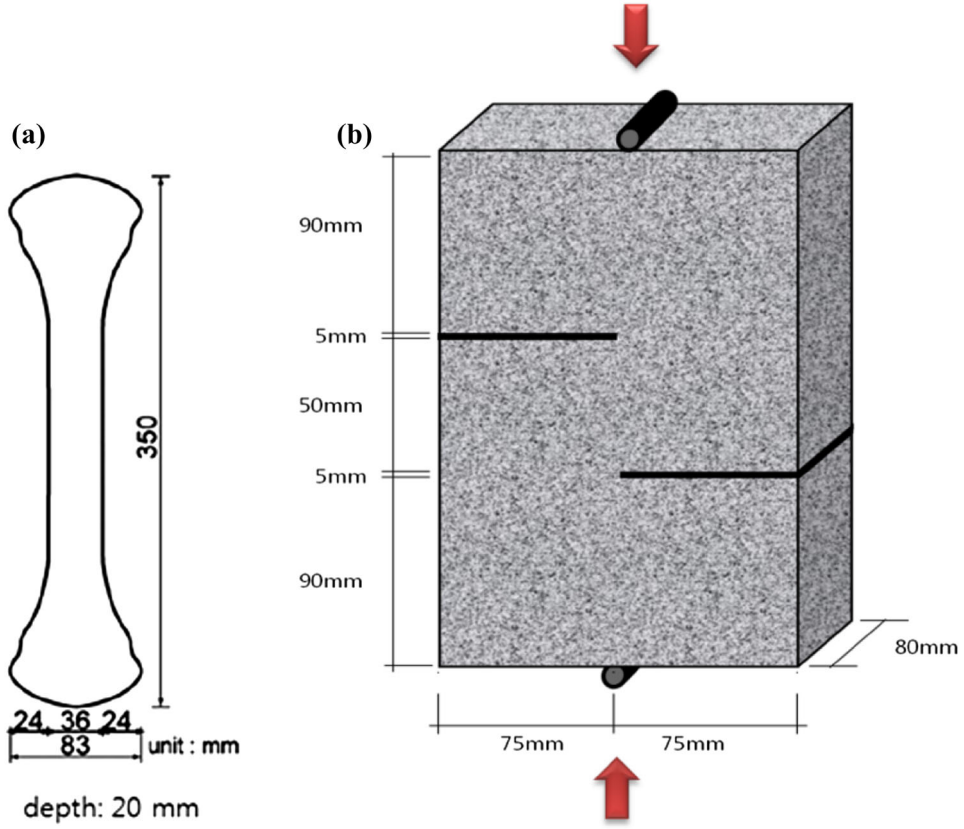

Fig. 2 Schematic of specimens for **a** direct tensile and **b** shear transfer strength test.

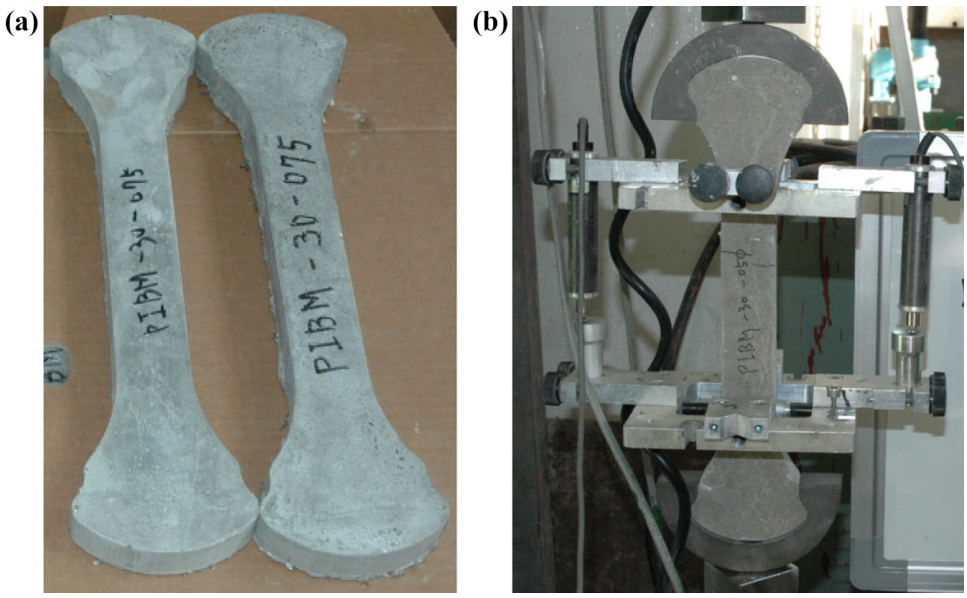

Fig. 3 Photos of **a** specimen and **b** test setup for direct tensile test.

elongation was measured by two linear variable differential transducers (LVDT) attached to both sides of the center of the specimen with a gage length of 150 mm as referred to the distance. The test was monitored under displacement control with a loading speed of 0.1 mm/min. From the direct tensile test, the tensile stress–strain curves were measured additionally with tensile strength and ultimate ductile tensile strain for two specimens for each mix.

For measuring the shear strength, dimension of specimen for shear transfer was 240 × 150 × 80 mm. To measure shear transfer across a plane in the composite, as shown in Fig. 4, by applying a compressive load, the test unit was designed to fail in shear on the shear plane of 50 × 80 mm in the specimen. A shear crack was induced by increasing the axial load of the UTM and the shear strength was measured at the moment of failure caused by shear crack (Mattock and Hawkins 1972).

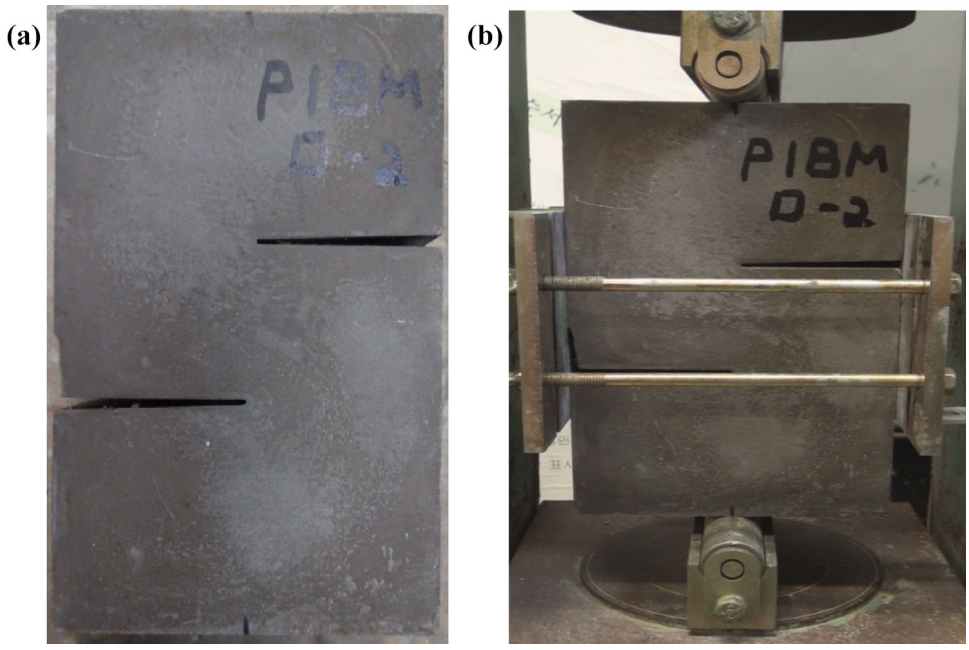

Fig. 4 Photos of **a** specimen and **b** test setup for shear transfer strength test.

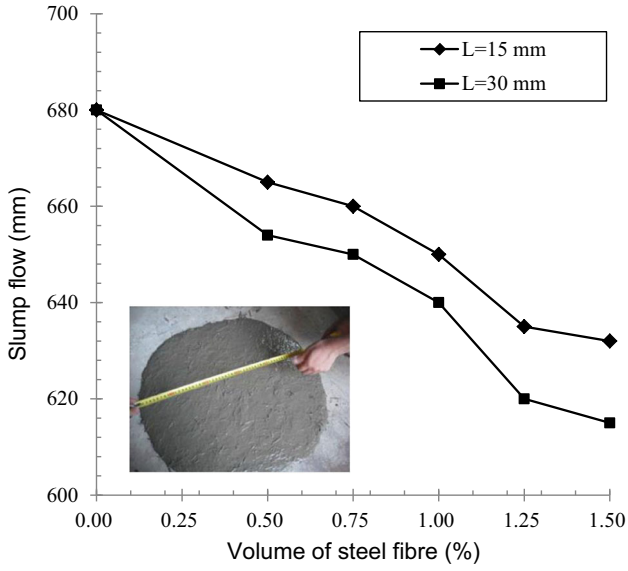

Fig. 5 Measured slump flow of AMS fibre cementitious composites for two fibre length of L = 15 mm and 30 mm.

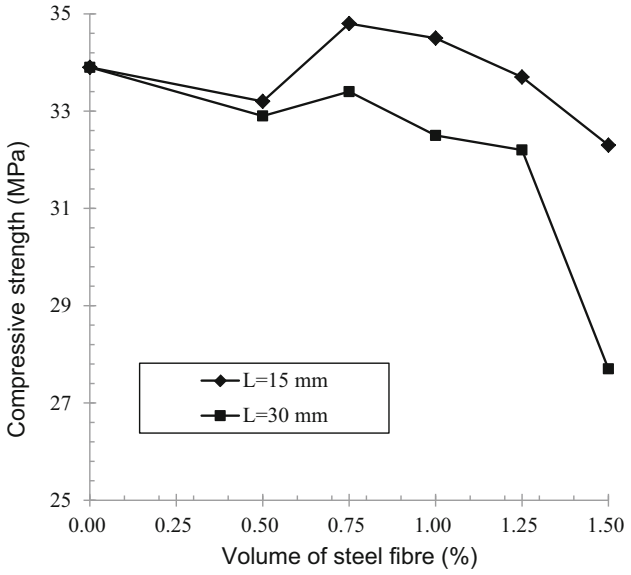

Fig. 6 Compressive strength of AMS fibre composites for two fibre length of L = 15 mm and 30 mm.

3. Characteristics of Slump Flow and Compressive Strength

The slump flow of mortar containing AMS fibre was measured as given in Fig. 5, together with a photo of measurement. It was evident that an increase in the volume of AMS fibre resulted in a decrease in the fluidity, irrespective of the length of the fibre. Fibre-free mortar had the slump flow, accounting for about 680 mm, whilst the fluidity was dramatically reduced by the AMS fibre. It may suggest that overwhelming amount of fibre is limited due to clash between the fluidity and strength development.

The compressive strength of mortar containing AMS fibre is given in Fig. 6. It was evident that the fibre might not benefit in enhancing the strength of concrete; there was only, in fact, a reduction of the compressive strength in the mix containing 30 mm long AMS fibre. In particular, the compressive strength at 1.5% of AMS fibre was equated to 27.7 MPa, whilst fibre-free mortar indicated 33.9 MPa. The variation in the compressive strength was again observed for 15 mm long AMS fibre: the range of the compressive strength was 32.3–34.8 MPa. Substantially, it seemed that no benefit in raising or at least sustaining the compressive strength was gained by AMS fibre in concrete. Above the fibre volume of 0.75%, the compressive strength tend to

reduce with increase of the fibre volume fraction which is mainly caused by insufficient fibre dispersion as observed in a literature (Yoo and Banthia 2017).

4. Test and Discussions on Direct Tensile Characteristics

After curing of 28 days, tensile behaviors of hardened AMS fibre composite were examined and test results were presented by tensile stress–strain curves as given in Fig. 7. Non-fibre mortar and AMS fibre-reinforced composite with a fibre volume of 0.5% were exempt from the direct tensile test due to a very high level of the brittleness in tension. In preliminary test, the tensile stress had been sharply dropped after the initial crack was generated when the tensile strain ranged from 0.22 to 0.23%. All specimens exhibit apparent multiple cracking patterns accompanying tensile strain softening and ductile behaviors with strain capacities ranging from 0.57 to nearly 0.75%. These ductile characteristics remain much higher than that in normal concrete and conventional FRC composites.

The tensile strength and strain simultaneously measured for each mixture are given in Figs. 8 and 9, respectively. It is clearly shown that an increase in the volume of the AMS fibre in mixture resulted in a mostly linear increase in the tensile strength, irrespective of the length of AMS fibre. The tensile strength of non-fibre mixture was equated to about 1.32 MPa, while the tensile strength of AMS fibre mixtures with the fibre volume of 1.0, 1.25 and 1.50% exceeded 4.0 MPa. Even with a lower volume of AMS fibre (i.e. 0.50 and 0.75%) the tensile strength was in the range of 2.46–3.57 MPa. When it comes to the tensile strain, it is also observed that an increase in the volume of AMS fibre in the mixture resulted in an increase in the tensile strain. In particular, with up to 0.75% of the AMS fibre in volume, the tensile strain was significantly increased by the AMS fibre, which was subsequently marginal in the variation in the strain, ranging from 0.57 to 0.75%. AMS fibre-reinforced cementitious composites may represent a post-cracked ductile strain in direct tensile test, which could not be observed in fibre-free concrete (Batson et al. 1972; Shah 1980). However the ductile capacity of AMS fibre-reinforced cementitious composites was reduced for ECC and SHCC mixes, imposing high ductile and strain-hardening characteristics in direct tensile post-cracked region as the maximum tensile strain was above 2.0% (Fischer and Li 2003; Lee et al. 2012; Choi et al. 2014; Cho et al. 2012). AMS fibres in cementitious mixture were expected to be fracture before complete pullout as shown in Fig. 10. This would cause a lower post-peak ductility compared to PVA fibres with a pullout failure.

When the ECC or/and SHCC were manufactured to mix PVA fibres into cementitious composites about 1.5–3.0% in volume of the mix, the tensile strength was not much affected (Fischer and Li 2003; Lee et al. 2012; Choi et al. 2014; Cho et al. 2012). From observations of current direct tensile test, it was supposed that AMS fibre-reinforced cementitious composites had ambivalent post-cracked tensile characteristics between steel fibre reinforced concrete and ECC mixture. For ductile post-cracked tensile strain capacities, the AMS fibre cementitious composite was superior to steel fibre reinforced concrete, but was inferior to ECC or SHCC mixtures, whilst the AMS fibre-reinforced cementitious composites could greatly enhance tensile strength, which cannot be observed in ECC or SHCC mixtures. Considering the fibre dispersion, mixtures at more than 1.5% fibre volume fraction were not recommendable to increase direct tensile strength as well as improve deformation capacities.

5. Test and Discussions on Shear Transfer Strength

After curing of 28 days, shear transfer capacity was examined to measure the shear strength. The shear crack was observed for all cases, as given in Fig. 11, together with the shear strength. It was clearly observed that an increase in the AMS fibre in the mix resulted in an increase in the shear strength, up to 1.25% of the AMS fibre in volume, irrespective of the length of fibre. In fact, the shear strength of the mixture with 1.25% of fibre in volume accounted for 11.77–11.20 MPa, while with 1.50% the shear strength ranged 9.30–9.77 MPa. The variation of shear strength for varying fibre contents was manifested as observed in a series of current test that AMS fibres mixed into cementitious composites were so efficient to promote the shear capacity of cementitious composites by suitable fibre contents. Mixtures of AMS fibre-reinforced cementitious composites exhibited up to 2.22 times and 2.35 times higher the average maximum shear strength than the mixture of non-fibre mortar, for the fibre length of 15 mm and 30 mm, respectively.

For mixtures with less than 1.25% fibre volume fraction, the shear strength was gradually increased according to the increase of fibre volume fraction because AMS fibres could be suitably dispersed into the cementitious mixture with below the fibre contents. A reduction in the shear strength with 1.50% fibre volume fraction was presumably due to a poor dispersion of fibres, which might get tangled and made fibre balls within cementitious mixtures. It could be commented from experiments that 1.0–1.25% fibre volume fractions were suitable to improve shear transfer capacity in AMS fibre-reinforced cementitious composites with the fibre length of 15 and 30 mm, and the mixtures with 1.25% fibre volume fraction could exhibit most excellent to develop shear transfer capacities in mixtures.

6. Conclusions

In the present study, a series of experimental programs was investigated to establish the feasibility of developing a new micro-steel fibre cementitious composite using OPC and GGBS mixing mortar and amorphous micro-steel fibres with

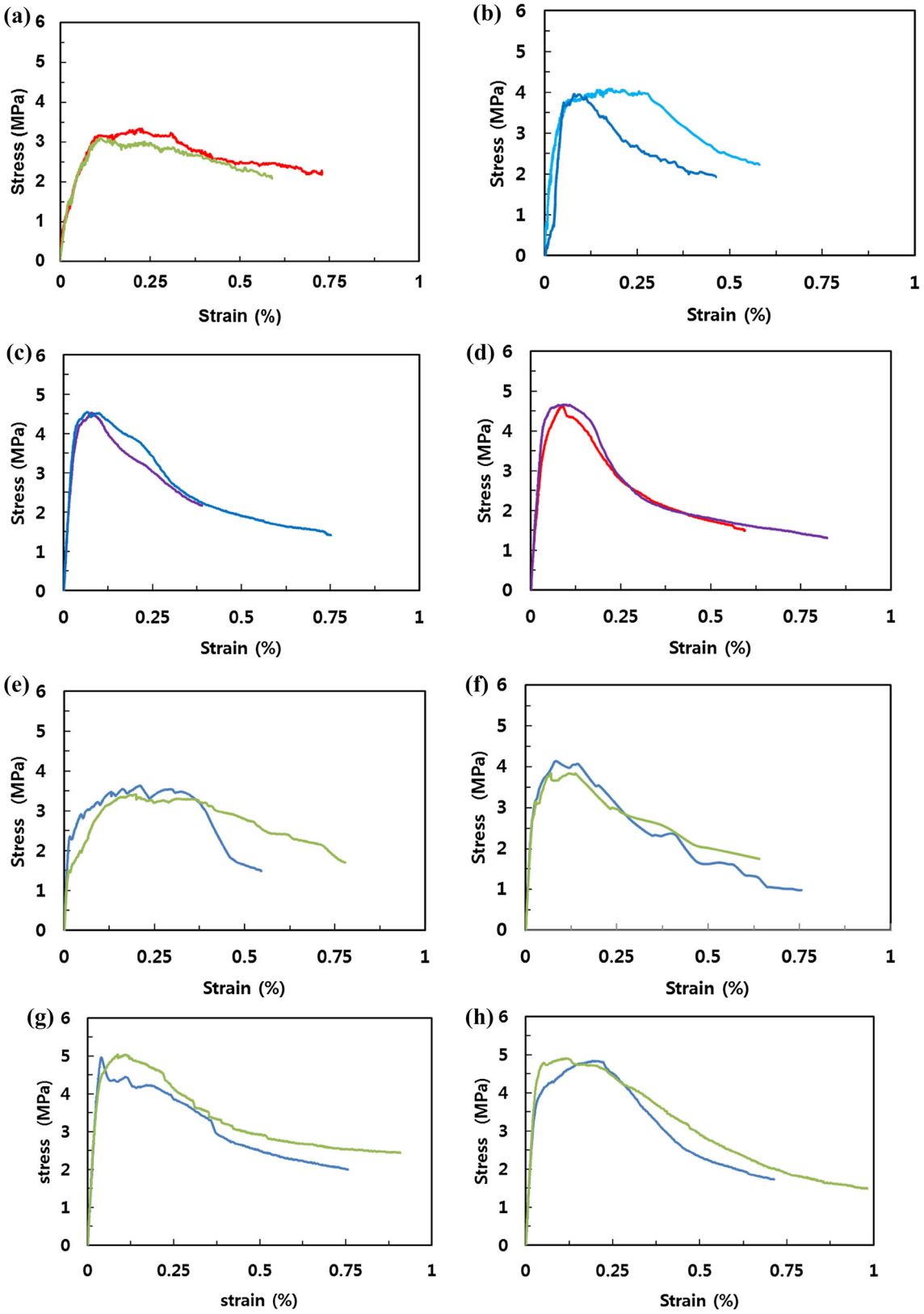

Fig. 7 Measured tensile stress and strain curves depending on the volume of steel fibre for two fibre length of L = 15 mm and 30 mm. **a** L = 15 mm (0.75%), **b** L = 15 mm (1.0%), **c** L = 15 mm (1.25%), **d** L = 15 mm (1.50%), **e** L = 30 mm (0.75%), **f** L = 30 mm (1.0%), **g** L = 30 mm (1.25%), **h** L = 30 mm (1.50%).

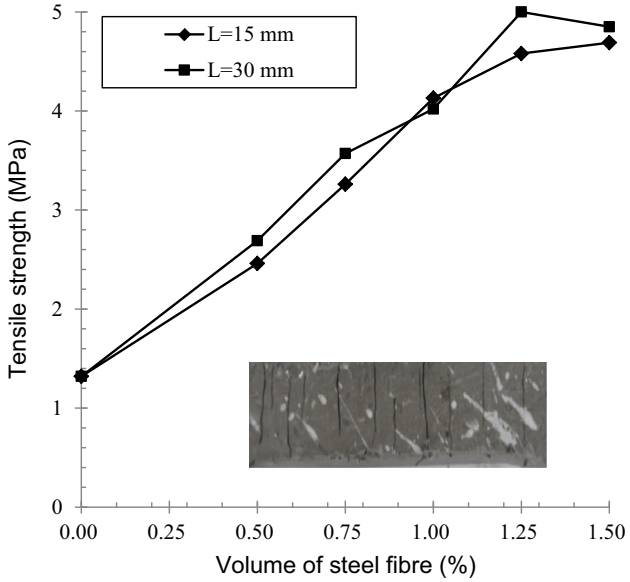

Fig. 8 Tensile strength of mortar containing steel fibre with the length of fibre together with a photo of tensile cracking after the test (Photo scale as a real length of 50 mm).

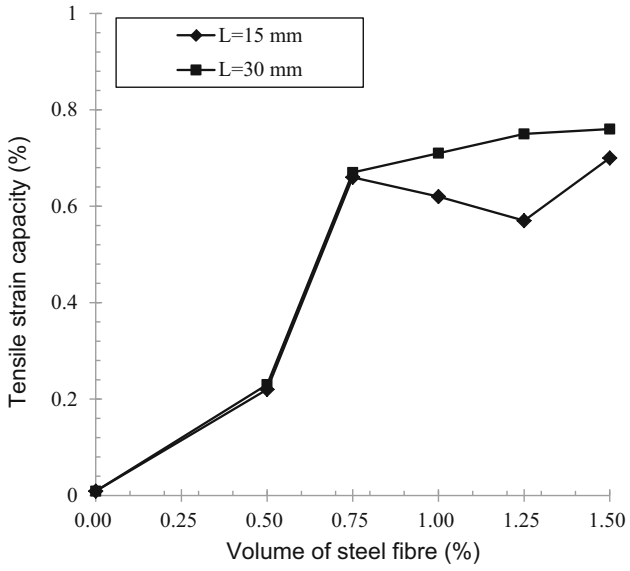

Fig. 9 Tensile strain of mortar containing steel fibre with the length of fibre.

Fig. 10 Fracture of fibres in tensile failure of AMS fibre cementitious composite.

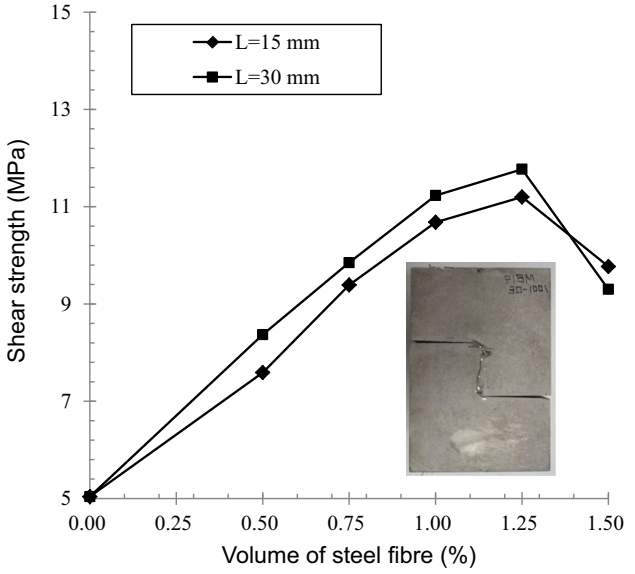

Fig. 11 Shear strength of mortar containing steel fibre depending on the length of the fibre together with an example of shear crack.

the length of 15 mm or 30 mm at 0.5–1.5% in volume, and the followings were concluded.

The flexible, light weighted properties of amorphous micro-steel fibres could allow excellent in flowable and disperable states of mixing with cementitious composites. The actual slump flow measured immediately after mixing was about 640 mm, as meeting the flowable workability for fresh concrete. It was increased the tensile strain and shear transfer strength of AMS fibre-reinforced cementitious composites by fiber bridging effects. The fibre dispersion seemed poor at exceeding 1.5% of AMS fibre in volume rather than lower values: the shear strength was adversely reduced at 1.5% of AMS fibre than at 1.25%. Moreover, the compressive strength seemed not affected by the fibre, whereas an increase in the fibre in the mix resulted in an increase in the tensile strength.

AMS fibre-reinforced cementitious composites had ambivalent post-cracked tensile characteristics between steel fibre reinforced concrete and ECC mixtures. For high ductile post-cracked tensile strain capacities, AMS fibre-reinforced cementitious composites was superior to steel fibre reinforced concrete but was inferior to ECC or SHCC mixtures. For the tensile strength, the ultimate tensile strength of AMS fibre-reinforced cementitious composites could be greatly enhanced varying with the fibre contents, as also observed in steel fibre reinforced concrete, but these phenomena of tensile strength enhancement cannot be fundamentally observed in ECC or SHCC mix.

Acknowledgements

This research was supported by a Grant (17RDRP-B076268-04) from Regional Development Research Program funded by Ministry of Land, Infrastructures, and Transport of Korean government, and supported by research fund from Chosun University, 2015.

References

Ashour, S. A., Hyasanain, G. S., & Wafa, F. F. (1992). Shear behavior of high-strength fiber-reinforced concrete beans without stirrups. *American Concrete Institute, 94,* 68–76.

ASTM. (2007). Standard test method for compressive strength of hydraulic cement mortars (using 50 mm [2 in.] cube specimens), ASTM C109/C109 M-07.

Batson, G., Jenkins, E., & Spatnet, R. (1972). Steel fibers as shear reinforcement in beams. *American Concrete Institute, 69,* 640–644.

Cho, C. G., Kim, Y. Y., Feo, L., & Hui, D. (2012). Cyclic responses of reinforced concrete composite columns strengthened in the plastic hinge region by HPFRC mortar. *Composite Structures, 94,* 2246–2253.

Choi, W. C., Yun, H. D., Cho, C. G., & Feo, L. (2014). Attempts to apply high performance fiber-reinforced cement composite (HPFRCC) to infrastructures in South Korea. *Composite Structures, 109,* 211–223.

De Hanai, J. B., & Holanda, K. M. A. (2008). Similarities between punching and shear strength of steel fiber reinforced concrete (SFRC) slabs and beams. *IBRACON, 1,* 1–16.

Dinh, N. H., Choi, K. K., & Kim, H. S. (2016). Mechanical properties and modeling of amorphous metallic fiber reinforced concrete in compression. *International Journal of Concrete Structures and Materials, 10*(2), 221–236.

Fischer, G., & Li, V. C. (2003). Design of engineered cementitious composites (ECC) for processing and workability requirement. *Portland, Proceedings of BMC, 7,* 29–36.

Kim, J. K., Kim, J. S., Ha, G. J., & Kim, Y. Y. (2007). Tensile and fiber dispersion performance of ECC (engineered cementitious composites) produced with ground granulated blast furnace slag. *Cement and Concrete Research, 37*(7), 1096–1105.

Kim, Y. Y., Lee, B. Y., Bang, J. W., Han, B. C., Feo, L., & Cho, C. G. (2014). Flexural performance of reinforced concrete beams strengthened with strain-hardening cementitious composite and high strength reinforcing steel bar. *Composites: Part B, 56,* 512–519.

Kim, D. J., Naaman, A. E., & El-Tawil, S. (2009). High performance fiber reinforced cement composites with innovative slip hardening twisted steel fibers. *International Journal of Concrete Structures and Materials, 3*(2), 119–126.

KS F 2402. (2007). Method of test for slump of concrete, Korea Standard Association.

Lee, B. Y., Cho, C. G., Lim, H. J., Song, J. K., Yang, K. H., & Li, V. C. (2012). Strain hardening fiber reinforced alkali-activated mortar—A feasibility study. *Construction and Building Materials, 37,* 15–20.

Li, V. C., Mishra, D. K., & Wu, C. (1995). Matrix design for pseudo strain-hardening fiber reinforced cementitious composites. *Materials and Structures, 28*(183), 586–595.

Lim, W. Y., & Hong, S. G. (2016). Shear tests for ultra-high performance fiber reinforced concrete (UHPFRC) beams with shear reinforcement. *International Journal of Concrete Structures and Materials, 10*(2), 177–188.

Lu, L., Tadepalli, P. R., Mo, Y. L., & Hsu, T. T. C. (2016). Simulation of prestressed steel fiber concrete beams subjected to shear. *International Journal of Concrete Structures and Materials, 10*(3), 297–306.

Mattock, A. H., & Hawkins, N. M. (1972). Shear transfer in reinforced concrete—Recent research. *PCI Journal, 17*(2), 55–75.

Morga, D.R., Heere, R., McAskill, N., & Chan, C. (1999). Comparative evaluation of systemductility of mesh and fibre reinforced shotcretes. In: Engineering foundation, New York sponsored conference shotcrete for underground support VIII campus do Jordao (pp. 1–23), Brazil.

Narayanan, R., & Darwish, I. Y. S. (1987). Use of steel fibers as shear reinforcement. *American Concrete Institute, 84,* 216–227.

Özcan, D. M., Bayraktar, A., Sahin, A., Haktanir, T., & Türker, T. (2009). Experimental and finite element analysis on the steel fiber-reinforced concrete(SFRC) beams ultimate behavior. *Construction and Building Materials, 23*(2), 1064–1077.

Özgür, E., & Khaled, M. (2009). Effects of limestone crusher dust and steel fibers on concrete. *Construction and Building Materials, 23*(2), 981–988.

Redon, C., & Chermant, J. L. (1999). Damage mechanics applied to concrete reinforced with amorphous cast iron fibers, concrete subjected to compression. *Cement & Concrete Composites, 21*(3), 197–204.

Seo, Y. S. (2006). Materials for machine (pp. 359–361), Gijeon.

Shah, S. P. (1980). Static and fatigue properties of concrete beams reinforced with continuous bars with fibers. *American Concrete Institute, 77,* 36–43.

Won, J. P., Hong, B. T., Choi, T. J., Lee, S. J., & Kang, J. W. (2012). Flexural behavior of amorphous micro-steel fibre-reinforced cement composites. *Composite Structures, 94,* 1443–1449.

Won, J. P., Hong, B. T., Lee, S. J., & Choi, S. J. (2013). Bonding properties of amorphous micro-steel fibre-reinforced cementitious composites. *Composite Structures, 102,* 101–109.

Yoo, D. Y., & Banthia, N. (2017). Experimental and numerical analysis of the flexural response of amorphous metallic fiber reinforced concrete. *Materials and Structures, 50*(1), 64–77.

Yoo, D. Y., Banthia, N., Yang, J. M., & Yoon, Y. S. (2016). Size effect in normal- and high- strength amorphous metallic and steel fiber reinforced concrete beams. *Construction and Building Materials, 121,* 676–685.

Yoo, D. Y., & Yoon, Y. S. (2016). A review on structural behavior, design, and application of ultra-high-performance fiber-reinforced concrete. *International Journal of Concrete Structures and Materials, 10*(2), 125–142.